Redox conditions of shallow seawater across the Ediacaran–Cambrian transition: Insights from trace elements, REE, and eustatic changes

Article *in* Geochemical journal GJ · July 2020

DOI: 10.2343/geochemj.2.0607

CITATIONS
0

READS
209

4 authors:

Yang Yang
Chinese Academy of Sciences
1 PUBLICATION **0** CITATIONS
SEE PROFILE

Wen Hanjie
Chinese Academy of Sciences
149 PUBLICATIONS **1,942** CITATIONS
SEE PROFILE

Jie Liu
Seismological Bureau of Shaanxi Province
4 PUBLICATIONS **52** CITATIONS
SEE PROFILE

Jeffrey de Fourestier
East China University of Technology
67 PUBLICATIONS **112** CITATIONS
SEE PROFILE

Geochemical Journal, Vol. 54, pp. 365 to 379, 2020 doi:10.2343/geochemj.2.0607

Redox conditions of shallow seawater across the Ediacaran-Cambrian transition: Insights from trace elements, REE, and eustatic changes

YANG YANG,[1,2] HANJIE WEN,[1,2]* JIE LIU[3] and DE FOURESTIER JEFFREY[4]

[1]State Key Laboratory of Ore Deposit Geochemistry, Institute of Geochemistry, Chinese Academy of Sciences, Guiyang 550081, P.R. China

[2]University of Chinese Academy of Sciences, Beijing 100049, P.R. China

[3]Shaanxi Earthquake Agency, Xi'an 710068, P.R. China

[4]State Key Laboratory of Nuclear Resources and Environment (East China University of Technology), Nanchang 330013, P.R. China

(*Received March 17, 2020; Accepted July 4, 2020*)

To explore the shallow marine redox state from the Ediacaran to the Cambrian (*ca*. 635–488.3 Ma) Yangtze Platform in southern China, this study presents traditional rare-earth element (e.g., δCe, δEu, REE distribution pattern and Y/Ho), enrichment factor, and paleoenvironment proxy data from the Kaiyang shelf from Nantuo to Loushanguan Formations. Our data from a drill core from Kaiyang suggest the occurrence of a fluctuating redox state from the Ediacaran to the Cambrian ocean, in which the fluctuating redox state of shallow water coexisted with eustatic change. We observe an obvious oxygenation signal of seawater during Ediacaran-Cambrian transition and a distinctive redox state in Ediacaran and Cambrian shallow seawater. We posit that the large-scale oxygenation of the atmospheric-oceanic system may have played a critical role in the main phase of Cambrian Explosion, and a fluctuating redox state of shallow seawater existed at the Cambrian stage.

Keywords: redox state, Ediacaran-Cambrian transition, trace elements, REE, eustatic change

INTRODUCTION

The Ediacaran-Cambrian transition was a crucial period in the history of the Earth. Many important geological events, such as the oxygenation event (called "Neoproterozoic oxygenation event") (Shields-Zhou and Och, 2011; Och and Shields-Zhou, 2012), occurred during this period, and major changes in continental configuration, global climate, and biological evolution and a range of variations in the system of oceanic-atmospheric chemical composition were observed (Amthor *et al*., 2003; Berner *et al*., 2003; Landing, 2004; Guo *et al*., 2007; Schroder and Grotzinger, 2007). Many studies in the past decade focused on the redox state of the paleo-ocean environment in the Ediacaran-Cambrian transition. Several of them suggested that oxygenated deep ocean water was widespread during the Late Neoproterozoic and triggered the evolution of the Ediacaran biota and Cambrian Explosion (Fike *et al*., 2006; Canfield *et al*., 2007; Scott *et al*., 2008). On the contrary, recent studies conducted with Fe-Mo-C-S systematics point to a marine redox stratification model in Ediacaran-Cambrian transitional oceans (Li *et al*., 2010; Feng *et al*., 2014; Chang *et al*., 2018). Several of these studies used the method of non-traditional isotopic geochemistry and obtained similar conclusions; Mo isotopic data suggested that the redox-stratified state may have lasted until the Early Cambrian (Wille *et al*., 2008; Wen *et al*., 2011; Xu *et al*., 2012). Xiang *et al*. (2017) reported that the expansion of oxic water in the global ocean postdates the main phase of Cambrian diversification (Cambrian Series 2, Stage 3), a result that is in conflict with those of several previous studies. In sum, the redox state of the ocean during the Ediacaran-Cambrian transition remains unclear.

During the Ediacaran-Cambrian transition period, two crucial episodes of marine phosphogenesis occurred worldwide and formed many phosphate deposits in Neoproterozoic and Cambrian (Cook and Shergold, 1984; Cook, 1992; Kholodov and Butuzova, 2001). Previous studies have shown that these phosphorus-bearing strata were deposited after "Snowball Earth." Planavsky *et al*. (2010) suggested that the significantly elevated marine phosphorus concentrations that followed "Snowball Earth" glaciations would have caused widespread phosphogenesis. Mi *et al*. (2010) indicated that the formation of phosphorites was related to changes in the

*Corresponding author (e-mail: wenhanjie@vip.gyig.ac.cn)

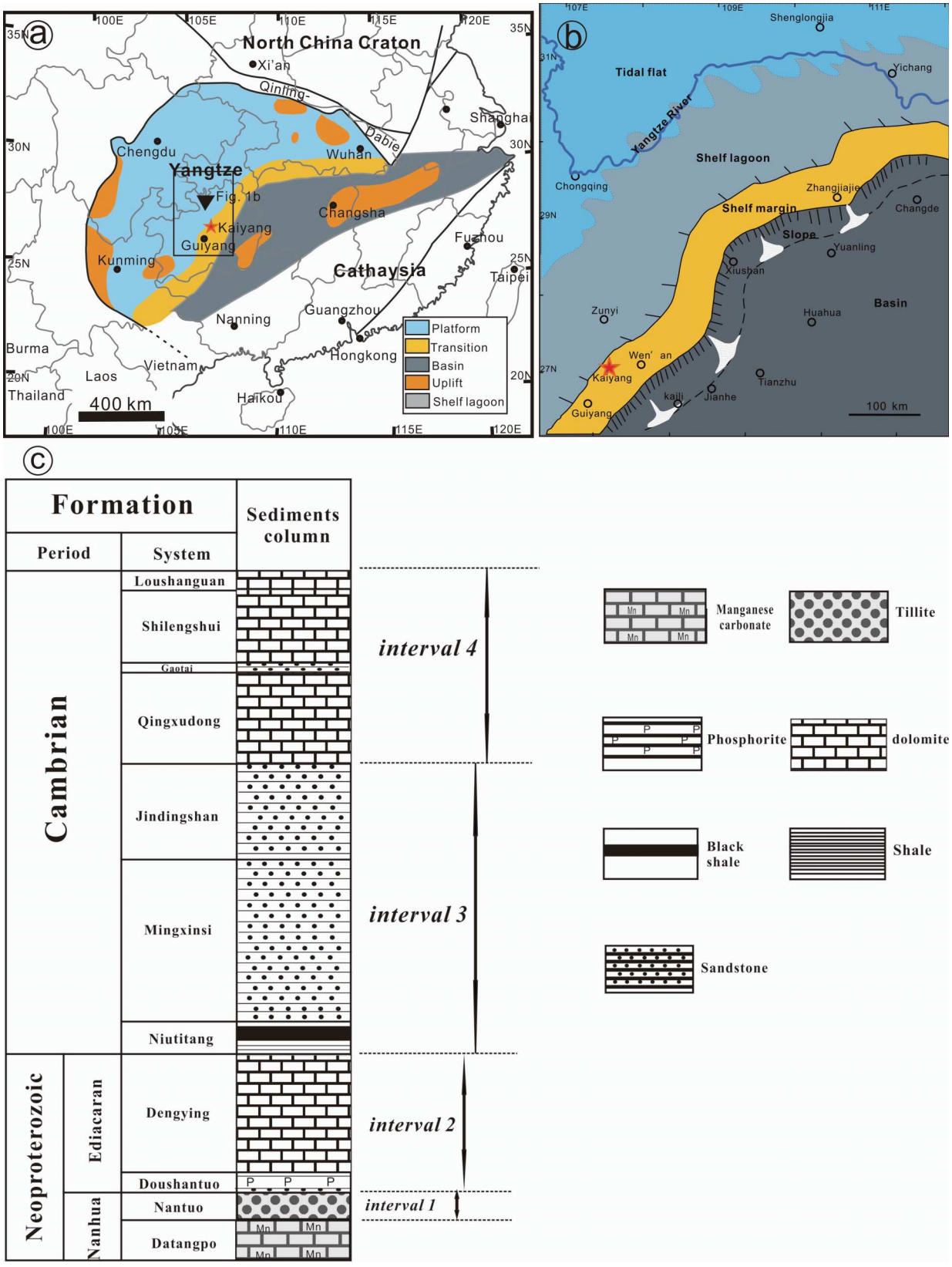

Fig. 1. Simplified paleogeographic map of the Yangtze Platform during the late Ediacaran to the earliest Cambrian (modified from Lehmann et al.,2016, Jiang et al.,2011, respectively). The stars refer to core sections studied in the study.

paleo-oceanic and ecological environment after "Snowball Earth." Therefore, phosphorites could contain extensive geochemical information on coeval ocean chemistry and can be used to reconstruct oceanic and biological evolution at the geological time scale (Jiang *et al*., 2007; Zhu *et al*., 2014). Meanwhile, carbonate is an important indicator for the reconstruction of the paleo-oceanographic environment because of its wide distribution in geological history, and it can represent the paleo-oceanographic chemical state.

In conclusion, the geochemical characteristics of carbonate and phosphorites are useful in the reconstruction of the paleoenvironment. The current study aims to enhance geochemical information on carbonate and phosphorites during the Ediacaran-Cambrian transition and provide evidence for the reconstruction of the paleoenvironment in southern China.

To ascertain the oceanic redox conditions during the Ediacaran-Cambrian transition, this study investigated trace elements, redox-sensitive elements (RSEs), and rare-earth elements (REEs) present in phosphatic rock co-existing with dolostone in Kaiyang phosphorite deposit in southern China. The results revealed an obvious oxygenation signal of seawater and a fluctuating redox state of shallow seawater during the Ediacaran-Cambrian stages.

Geological Setting

The successions from late Ediacaran to early Cambrian are well preserved in the Yangtze Platform and represent different paleo-ocean gradient settings. Three distinct facies regions, namely, a platform facies, transition belt, and basin, can be distinguished from northwest to southeast, as illustrated in Figs. 1a and 1b (Steiner *et al*., 2001; Guo *et al*., 2007; Jiang *et al*., 2011; Lehmann *et al*., 2016).

A well-preserved stratigraphic succession, namely, Kaiyang section (shelf, 27°10′30″ N–27°12′38″ N, 106°52′41″ E–106°54′08″ E), located near Yongwen Village in Kaiyang County in northeastern Guizhou Province was selected for this study. Paleo-geographically, Kaiyang section is located on a carbonate platform reflecting shallow-water sedimentation, as documented by Zhu *et al*. (2007). It comprises the Ediacaran Nantuo, Doushantuo, and Dengying Formations and the Cambrian Niutitang, Mingxinsi, Jingdingshan, Qingxudong, Gaotai, Shilengshui, and Loushanguan Formations. The base of the Kaiyang location investigated in this work contains sandstone from the Ediacaran (Neoproterozoic) Nantuo Formation, which is conformably overlain by the Ediacaran Doushantuo Formation. Various rock types exist in Doushantuo Formation, and these types include phosphorite, siltstone, and dolomite. Dengying Formation is conformably overlain by Doushantuo Formation, in which dolomite is the typical rock type. Dengying Formation is disconformably overlain by Cambrian Niutitang Formation, and Liuchapo Formation has disappeared. This condition means that the rapid transgression in the rock sampled from Kaiyang occurred during Ediacaran-Cambrian transition. Niutitang Formation contains dolomite, carbonaceous shale, and silicate rocks. Mingxinsi, Jingdingshan, and Gaotai Formations consist mainly of clastic rocks, such as sandstone and siltstone. Qingxudong, Shilengshui, and Loushanguan Formations are composed mainly of dolomite.

In accordance with the lithology of the study area, we divided the profile into four intervals. Interval 1 contained Nantuo Formation, Interval 2 contained Doushantuo and Dengying Formations, Interval 3 comprised Niutitang, Mingxingsi, and Jindingshan Formations, and Interval 4 was composed of Qingxudong, Gaotai, Shilengshui, and Loushanguan Formations. The stratigraphic sequence is described in Fig. 1c.

Samples and Methods

Fresh samples were collected from drill hole ZK313 at the Kaiyang phosphorous deposit in southern China, and the drilling depth was 1483.09 m. The formation thickness from which the rock samples were obtained was 1028–1514 m (1028 m is the minimum value of total formation thickness, and 1514 m is the maximum value of total formation thickness). We divided the profile into four intervals. Interval 1 (KY-472 to KY-490) contained sandstone. Interval 2 (KY-346 to KY-471) consisted of phosphorite, siltstone, and dolomite, among which dolomite was the typical rock type. Interval 3 (KY-116 to KY-345) contained dolomite, carbonaceous shale, and clastic rocks, and Interval 4 (KY-2 to KY-115) consisted mainly of dolomite. A total of 434 samples were analyzed for major and trace elements. Prior to the geochemical analysis, each sample was cleaned with distilled water, dried, and crushed to 200 mesh.

The major and trace elements in the samples were analyzed through X-ray fluorescence and inductively coupled plasma mass spectrometry, respectively, at ALS Chemex (Guangzhou) Co., Ltd. The analytical uncertainty for the elemental concentrations was generally better than 5%.

The enrichment factors were calculated with the equation $X_{EF} = [(X/Al)_{sample}/(X/Al)_{PAAS}]$ (e.g., Tribovillard *et al*., 2006, 2012; Algeo and Tribovillard, 2009). We chose post-Archean Australian shale (PAAS) data, which were obtained from the work of McLennan (2001), for normalization. The Al concentration in our samples was low. Therefore, we selected Zr for normalization (equation: $X_{EF} = [(X/Zr)_{sample}/(X/Zr)_{PAAS}]$).

Ce and Eu anomalies were calculated with the equations $\delta Ce = Ce_n/(La_n*Pr_n)^{1/2}$ and $\delta Eu = Eu_n/(Sm^2{}_n*Tb_n)^{1/3}$,

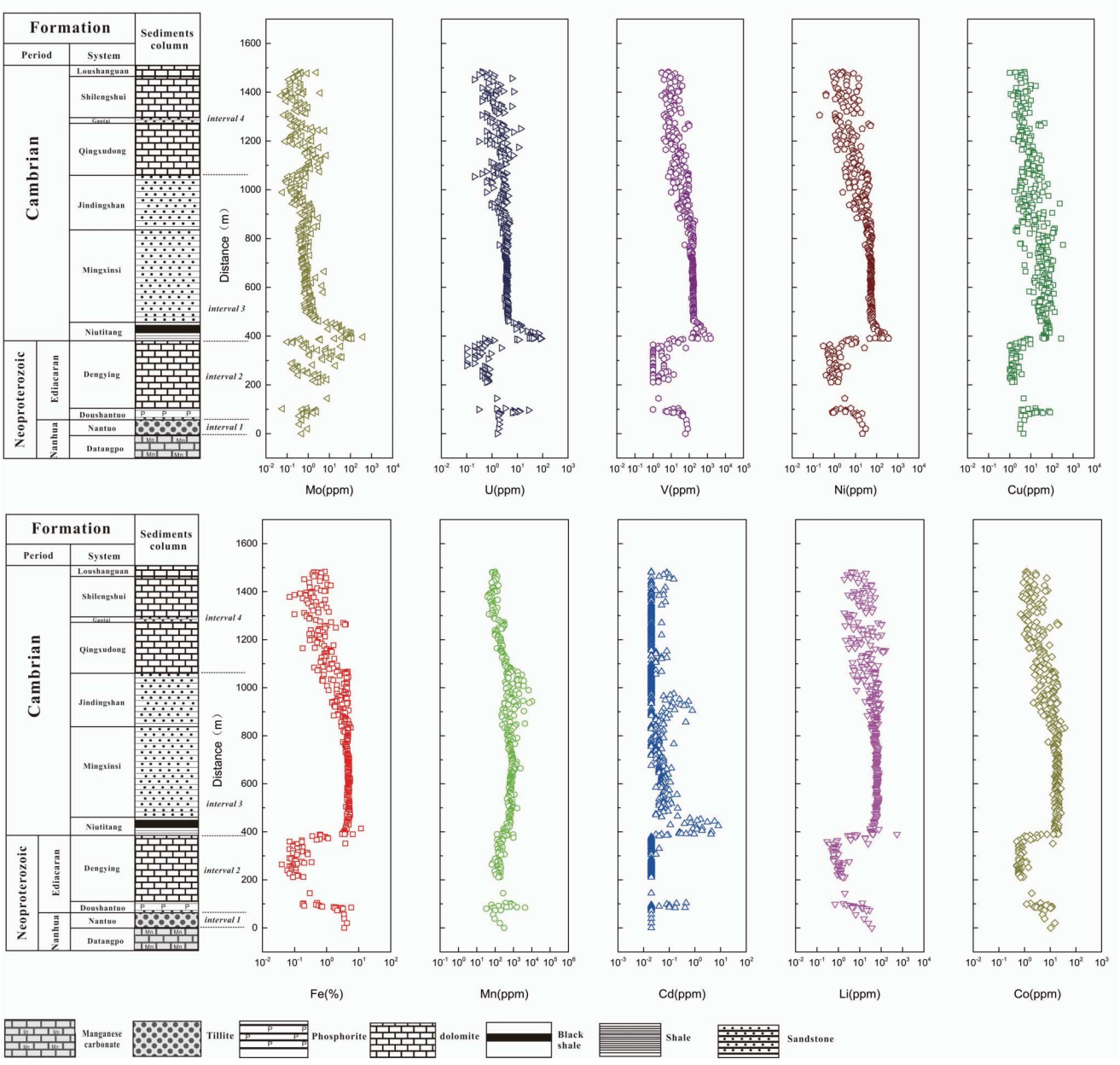

Fig. 2. The concentrations of RSEs, Fe and Mn.

respectively, which were obtained from the work of Lawrence and Kamber (2006). In the equations, the subscript n de-notes the normalization of concentrations against PAAS (McLennan, 1989).

RESULTS

Major and trace elements

The major and trace elements in the samples are shown in Supplementary Tables S1 and S2 and Fig. 2. Distinct elemental concentrations were observed in different intervals in the study area. The samples from Nantuo Formation (Interval 1) contained highly variable Mn, Li, and Co concentrations; the values ranged from 94 ppm to 310 ppm for Mn (mean 153 ± 96 ppm), from 6.5 ppm to 36.7 ppm for Li (mean 21.0 ± 11.2 ppm), and from 5.0 ppm to 15.1 ppm for Co (mean 8.5 ± 4.2 ppm). In this interval, Fe, Mo, U, V, Ni, Cd, and Cu were relatively homogeneous and had mean concentrations of 3.4 ± 0.8%, 0.53 ± 0.23 ppm, 1.78 ± 0.13 ppm, 66.8 ± 14.3 ppm, 20.2 ± 6.5 ppm, 0.02 ppm, and 4.24 ± 1.06 ppm, respectively. The sandstones from Interval 3 showed a similar change in

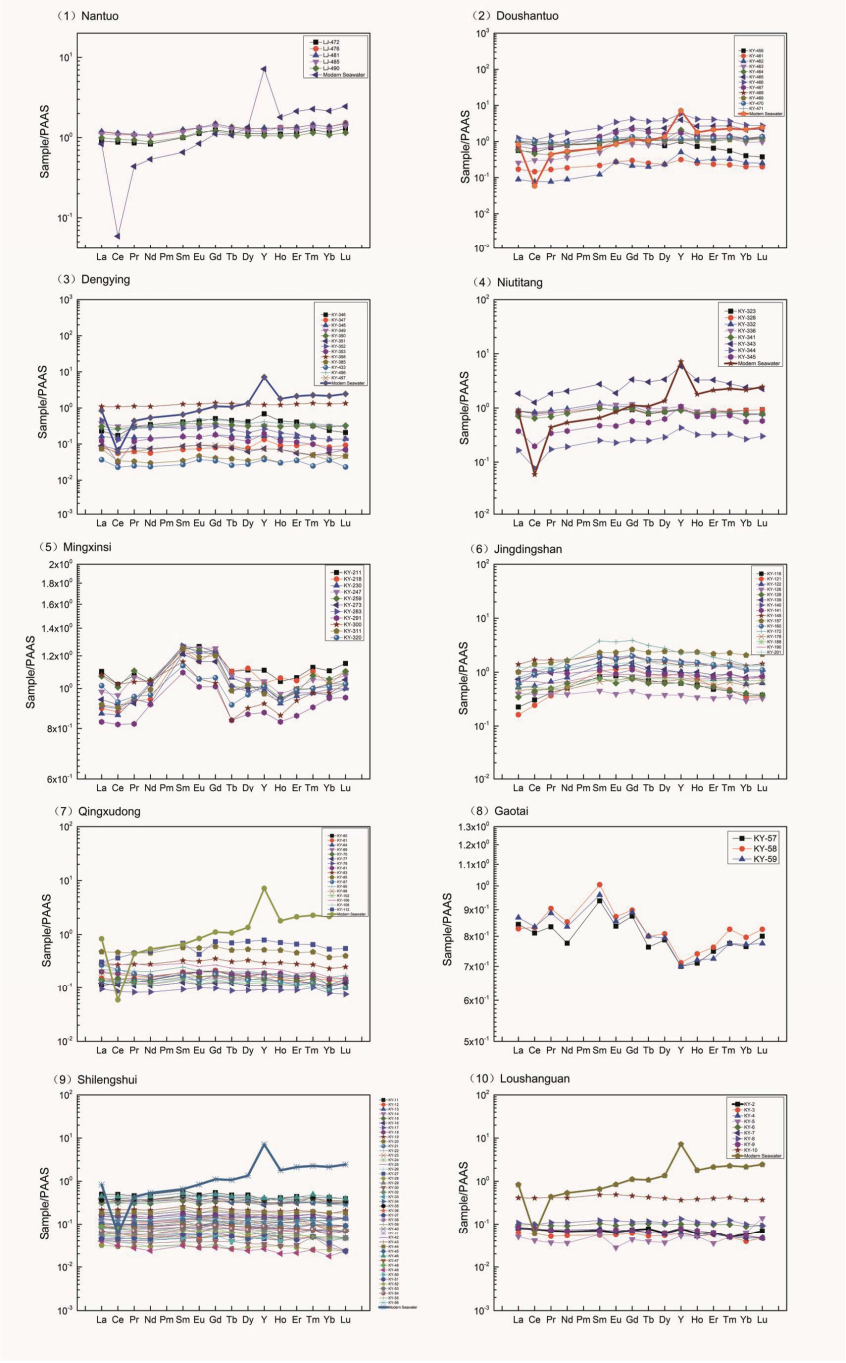

Fig. 3. REE patterns of the different strata of the Kaiyang.

element concentration as Interval 1. Black shale from Interval 3 (Niutitang Formation) exhibited multi-element enrichment, especially RSEs. High concentrations of V (mean 426 ± 362 ppm), Ni (mean 134 ± 85 ppm), U (mean 33.0 ± 24.1 ppm), Mo (mean 65.4 ± 76.7 ppm), and Cu (mean 60.1 ± 47.5 ppm) were found in this interval. Intervals 2 and 4 were dominated by carbonates, but their element concentrations differed. The carbonates from Interval 2 had a higher concentration of Mo (mean 4.87 ± 8.27 ppm) than the carbonates in Interval 4, but the concentrations of V (mean 5.20 ± 7.13 ppm), Ni (mean 1.86 ± 2.02 ppm), U (mean 1.26 ± 3.90 ppm), Cu (mean 3.22 ± 5.33 ppm), and Li (mean 1.93 ± 2.97 ppm) were lower than those in interval 4 (mean 16.6 ± 13.1 ppm, 5.67 ± 4.82 ppm, 2.0 ± 2.1 ppm, 6.9 ± 6.7 ppm, 21.2 ± 27.8 ppm, respectively).

REEs

In the four intervals, the ∑REE values obviously changed (mean 228 ppm, 117 ppm, 199 ppm, 48 ppm, respectively), and the ∑REE values conformed to the general rule of gradually decreasing from argillaceous rock to clastic rock to carbonates (argillaceous rock: 205 ppm, clastic rock: 194 ppm, and carbonates: 58.9 ppm).

The REE distribution pattern in the study area (Fig. 3) could be roughly divided into three types as follows: (1) HREE enrichment, left-leaning type (e.g., Nantuo, Doushantuo, and Niutitang Formations); (2) flat type [Dengying (several samples) and Qingxudong Formations]; and (3) MREE enrichment (Mingxinsi, Jindingshan, and Gaotai Formations).

No significant Ce (mean of 0.99, 0.88, 0.99, and 1.00) and Eu (mean of 1.08, 1.29, 1.00, and 0.95) anomalies were observed in the four intervals. However, Dengying and Niutitang Formations had a significant negative Ce anomaly (0.31 and 0.50, respectively), and the carbonates from Interval 2 showed a lower negative Ce anomaly (mean 0.8) than those in Interval 4 (mean = 1). This result suggests that the paleoseawater in Interval 2 was more oxidized than that in Interval 4. In Interval 2 (Doushantuo Formation), a positive Eu anomaly (maximum of 1.90) was observed. Interval 2 contained the highest Y/Ho ratio (mean of 42.3), and Intervals 1, 3, and 4 were relatively homogeneous with mean Y/Ho ratios of 26.4, 28.6, and 28.4, respectively. The carbonates from Interval 2 had a higher Y/Ho ratio (mean = 44.3) than those in Interval 4 (mean = 28.8).

Discussion

Disturbance of detrital origin

We evaluated whether an element is controlled by detrital flux or the influence of burial and diagenesis after deposition on REE partition type. Shields and Stille (2001) suggested that the influence of burial and diagenesis after deposition on REE partition type can be detected using the negative correlation between Ce anomaly and Dy_N/Sm_N (Fig. 4). If they have a negative correlation, then REE cannot be used to trace the paleoenvironment.

We did not find a negative correlation between Ce anomaly and Dy_N/Sm_N in the carbonates and phosphorites, indicating that our REE geochemistry proxy recorded primary information of ancient seawater.

To confirm whether an element is controlled by detrital flux, we determined the correlation coefficient between the given element and Al or Ti. A positive correlation indicates that the element is disturbed by detrital materials (Tribovillard *et al*., 2006). The Al concentration in our samples was low; therefore, we selected Zr to trace the influence of the detrital components. The correlation between redox-sensitive elements, total REE, and Zr are described in Figs. 5 and 6. In our studied samples, an absence of positive correlation was observed among ∑REE, Mo, U, V, Ni, Cu, and Zr from shales, carbonates, and phosphorites. However, sandstone and shales were affected by detrital components, indicating that elements from carbonates and phosphorites can be used as proxies for our study.

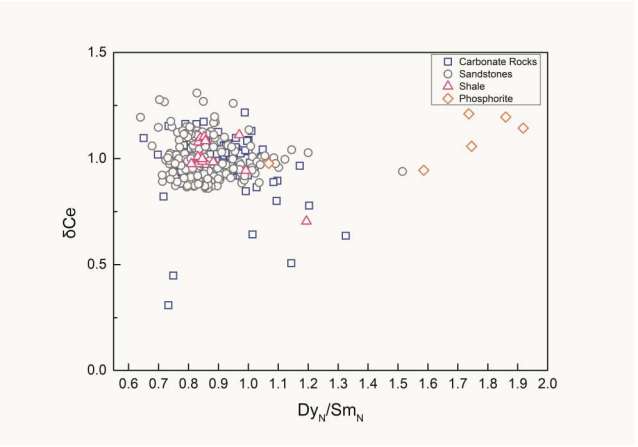

Fig. 4. The correlation between Ce anomaly and Dy_N/Sm_N.

REE geochemistry in carbonates and phosphorites

Interpretation of the observed Ce and Eu anomalies Ce can exist in either Ce^{3+} or Ce^{4+} form depending on the redox conditions. In modern oxygenated seawater, Ce^{3+} is oxidized to Ce^{4+} form through mediation by Mn oxides and/or bacteria (Byrne and Sholkovitz, 1996; Takahashi *et al*., 2000; Ohta and Kawabe., 2001; Tanaka *et al*., 2010). Ce^{3+} adsorbed on Mn oxides and hydroxides is preferentially oxidized to Ce^{4+}, and Ce^{4+} is preferentially adsorbed and sequestered by Mn oxides and hydroxides (Elderfield *et al*., 1981; Bau *et al*., 1996; Tachikawa *et al*., 1999). The solubility of Ce^{3+} and Ce^{4+} differs, that is, Ce^{3+} is soluble, whereas Ce^{4+} is insoluble. Thus, in the ocean system, Fe-Mn sediments show relative enrichment in Ce and positive Ce anomalies; hence, oxygenated seawater exhibits corresponding negative Ce anomalies (Bau *et al*., 1996). Byrne and Sholkovitz (1996) suggested that the dissolved REE pattern exhibits strongly negative Ce anomalies (approximately 0.06–0.16) in modern fully oxygenated deep oceans, whereas Ce anomalies are weak or even absent in suboxic and anoxic oceans because of the reductive dissolution of settling Mn- and Fe-rich particles (German *et al*., 1991). Thus, we can trace the oxidation degree of oceans by using Ce anomalies. Ce anomalies, which are useful tracers, have been used to trace paleo-oceanic redox conditions (McArthur and Walsh, 1984; Dulski, 1994; Webb and Kamber, 2000; Shields and Stille, 2001; Nothdurft *et al*., 2004; Slack *et*

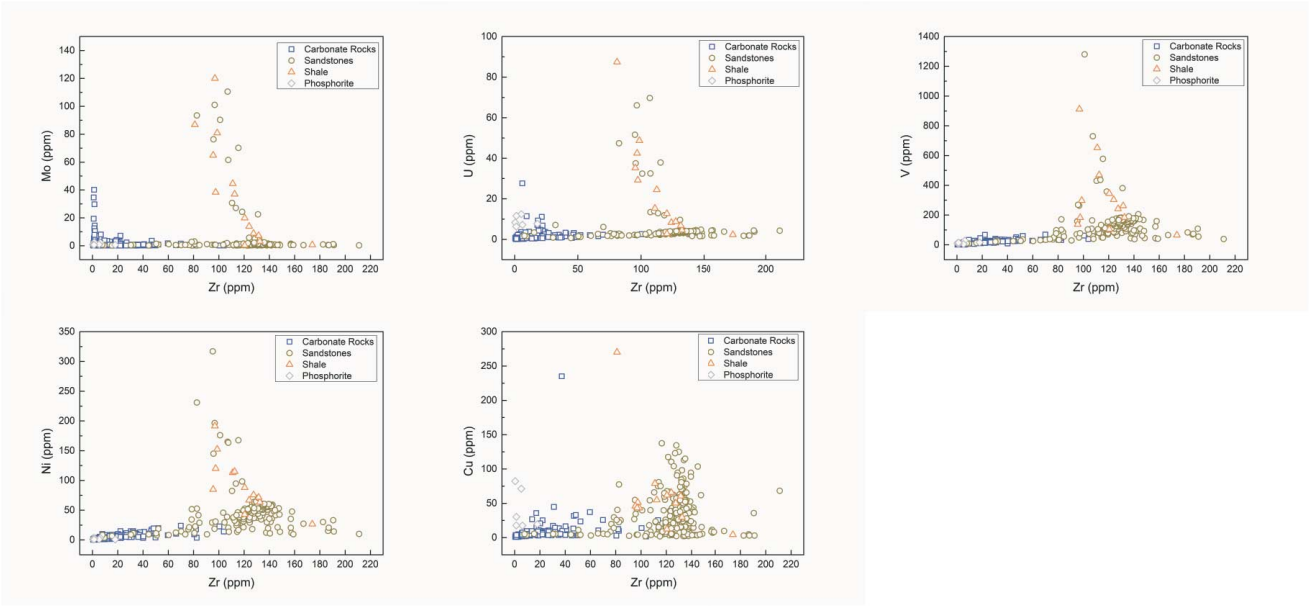

Fig. 5. The correlation between redox-sensitive elements and Zr.

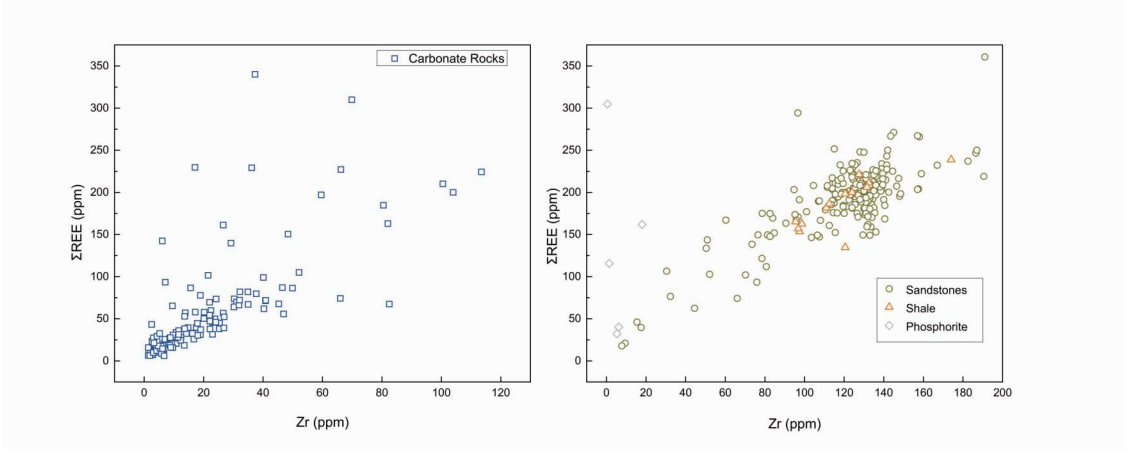

Fig. 6. The correlation of ∑REE and Zr. In our studied samples, carbonates and phosphorites were not affected by the detrital components.

al., 2007; Ling *et al*., 2013).

The variations of Y/Ho, δCe and δEu in the study area are described in Fig. 7. In our study, we found negative Ce anomalies in carbonates from Interval 2 (Dengying Formation), and the minimum value existed in the Interval 2–3 transition (upper Dengying Formation and lower Niutitang Formation) (approximately 0.30–0.50). In Doushantuo Formation, the δCe values of carbonates were between 0.90 and 1.00 (mean of 0.93) and correlated with the δCe values in the phosphorite bed. This result shows that the redox state of shallow water during the Doushantuo stage was anoxic. The δCe values decreased systematically from the bottom to the top of Dengying Formation. This decrement cannot be explained by the change in the depositional depth of the carbonates but suggests that shallow waters became increasingly oxygenated during this stage. The δCe values increased systematically (approximately 0.5–1.0) from the bottom to the top of the Niutitang Formation, and this situation continued until Loushanguan Formation. This finding indicates that the local water was oxidized gradually during Interval 2–3 transition. In Interval 4, the δCe values of carbonates were relatively homogeneous (0.89–1.22, mean = 1.00), showing that the local water from which the carbonates precipitated was relatively anoxic. Overall, the δCe values in Kaiyang area suggest that distinc-

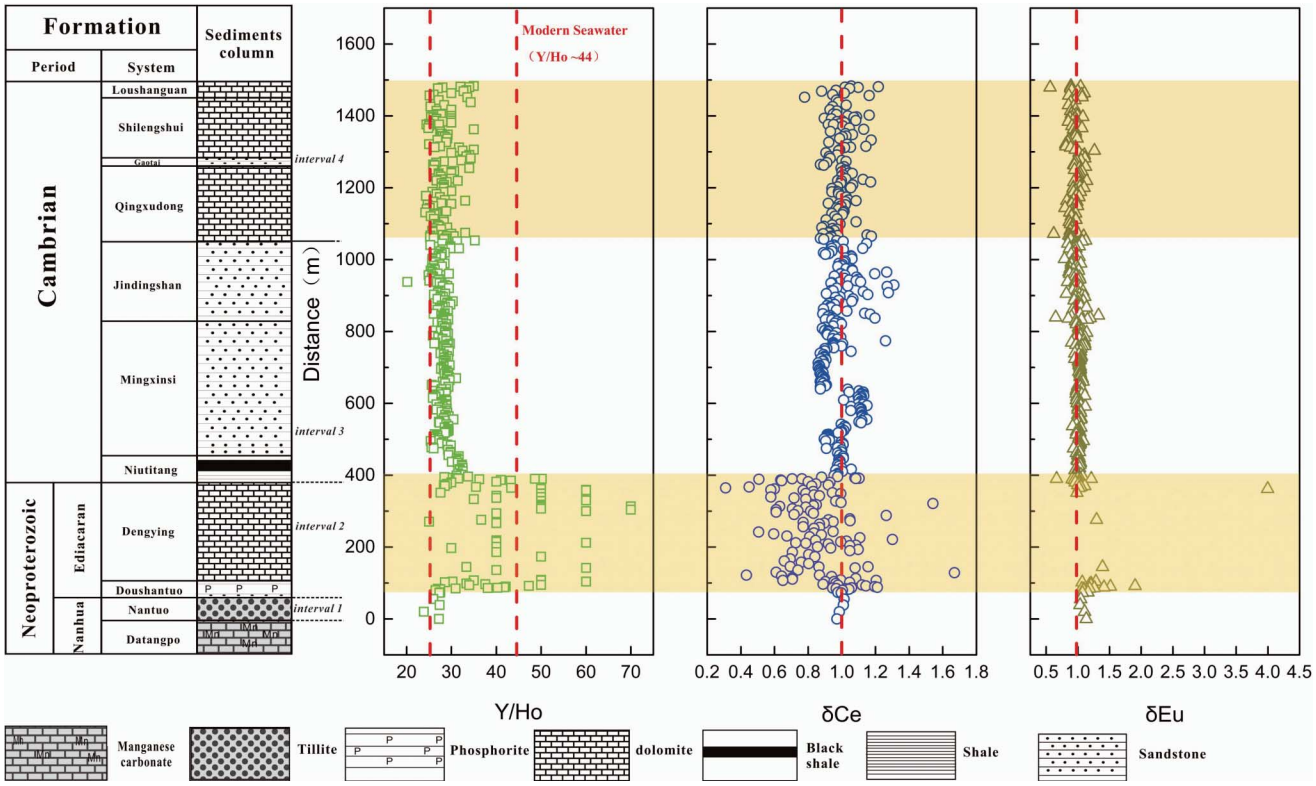

Fig. 7. Y/Ho, δCe and δEu of the Kaiyang Section. Yellow shadows refer to anomaly of Ce, Eu and Y/Ho in two carbonates intervals. (The vertical broken blue lines represent for boundary of negative/positive anomalies.)

tive shallow water existed in two intervals. The shallow water in Interval 2 was oxidized gradually, but the shallow water in Interval 4 became anoxic. Hence, the redox state of shallow seawater fluctuated.

In addition, Eu anomalies can be used to trace formations influenced by hydrothermal fluids. Many previous studies have suggested that hydrothermal fluids have similar REE patterns and positive Eu anomalies in different tectonic settings (e.g., Klinkhammer *et al*., 1994; Bau and Dulski, 1999; Douville *et al*., 1999). Therefore, we examined the possible influence of hydrothermal fluids.

We observed positive Eu anomalies in the phosphorite bed in Interval 2 (Doushantuo Formation) (approximately 1.2–1.9), which may indicate the involvement of hydrothermal fluids during its formation and the development of phosphate deposits. The remaining areas without positive Eu anomalies (~1.0) may be weakly or not influenced by hydrothermal fluids.

Y/Ho ratio Using previously established methods for the determination of Y and other REEs, Zhang *et al*. (1994) and Bau *et al*. (1996) showed that the oceanic distributions of Y closely resemble those of Ho because they have similar physical and chemical properties, such as being trivalent and having a similar ionic radius and electronegativity. However, the geochemical behavior of Y and Ho differs in various environments. Therefore, Y/Ho is an important proxy to trace the paleoenvironment. In an oxidized water environment, Ho shows preferential sorption in Fe- and Mn-oxyhydroxides compared with Y; it sinks to the seafloor and has an adsorption ratio that is nearly twice as high (Nozaki *et al*., 1997). Therefore, a high Y/Ho ratio (44–83) appears in an oxidized water environment (Bau *et al*., 1997; Nozaki *et al*., 1997).

In an anoxic water environment, because of the preferential sorption of Ho with respect to Y on Fe- and Mn-oxyhydroxides that eventually dissolve in anoxic water, an increase of Ho results in reduced water by as much as twice for Y; in turn, this situation causes a decrease in the Y/Ho value from 55 to 36 (Nozaki *et al*., 1997; Bau *et al*., 1997). The Y/Ho ratio in terrigenous clastic have a stable value (23–27), so terrigenous clastic can make the Y/Ho ratio decrease (Nozaki *et al*., 1997). The Y/Ho ratio (mass ratio) of PAAS is 27. Sediments or sedimentary rocks have a higher Y/Ho ratio than this value; their value is close to 44 (Y/Ho ratio of seawater), which indicates the absence or presence of only a small amount of terrigenous clastic contamination (Webb and Kamber, 2000).

In our study, we found the highest Y/Ho ratio in the carbonates from Interval 2 (approximately 29–70, mean

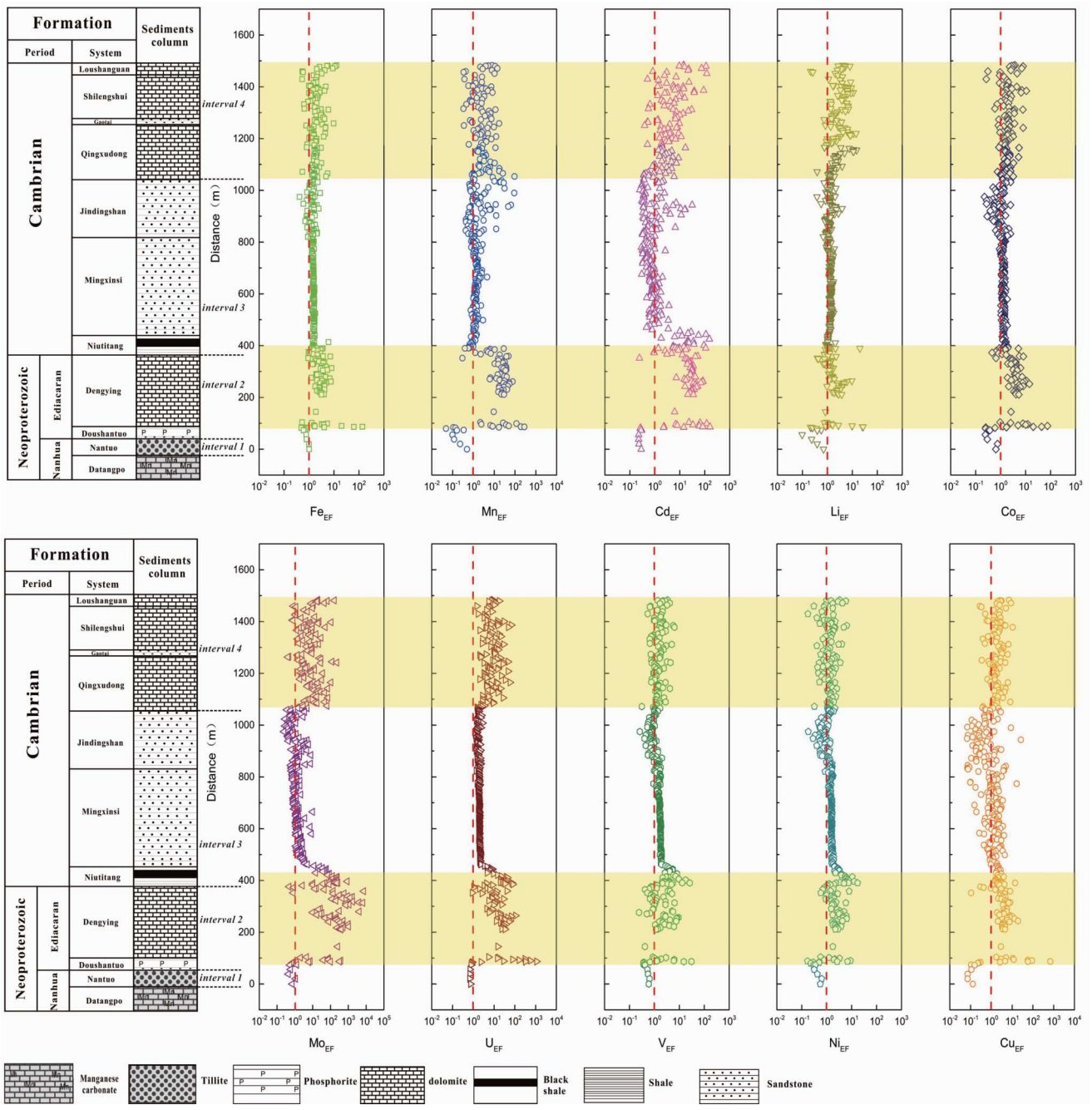

Fig. 8. Enrichment Factor of the Kaiyang Section. Yellow shadows refer to two episodes of obvious elements enrichment, and the pattern of them may be difference.

= 44), which suggests oxidized shallow seawater in this interval. In Interval 4, the Y/Ho ratio in the carbonates was lower than that in Interval 2 (approximately 25–35, mean = 29), which denotes relatively anoxic shallow seawater.

The Y/Ho ratios in the phosphorites from Doushantuo Formation (approximately 34–47, mean = 41, and only one sample had a Y/Ho ratio greater than 44) indicate that the local water from which the phosphorites precipitated was anoxic relative to Dengying Formation. Consequently, preferential sorption of Ho with respect to Y occurred on Fe- and Mn-oxyhydroxides that eventually dissolved in the anoxic water, causing a decrease in the Y/Ho value. The results of Y/Ho ratios were closely related to δCe.

REE distribution pattern REE is an important tool that is widely used in geochemical studies on ore deposits, oceans, and hydrothermal processes. In an oxic environment, the seawater column exhibits LREE and HREE depletion and HREE enrichment patterns of the left-leaning type because of scavenging particles (i.e., Fe-Mn oxyhydroxides or organic matter) (LREE > MREE > HREE) (Sholkovitz *et al*., 1994; Bau *et al*., 1996). In an anoxic water environment, the reduction and release of Fe-Mn hydroxide can lead to the enrichment of LREE and MREE in the bottom part of the water and HREE depletion relative to LREE and MREE.

In our samples, the shale-normalized REE patterns of phosphorite in Interval 2 (Doushantuo Formation) were characterized by HREE depletion relative to modern seawater (Dy_N/Yb_N value: average 1.08 ± 0.16, modern seawater: 0.8) and showed no Ce anomaly. This characteristic of Doushantuo phosphorite indicates that the marine depositional environment was anoxic.

The shale-normalized REE patterns of Interval 2–3 transition (Dengying and lower Niutitang Formations) exhibited a similar REE pattern as modern seawater and had negative Ce anomaly (approximately 0.3–0.7), suggesting that the marine depositional environment became increasingly oxygenated from Dengying Formation to the lower Niutitang Formation.

After Niutitang Formation, the Ce anomaly of the overlying strata obviously decreased, and some strata even had no Ce anomaly (approximately 0.99–1.27). All of them showed the characteristics of HREE depletion, indicating that the environment had become reductive.

The REE patterns of Interval 4 (Qingxudong, Shilegnshui, and Loushanguan Formations) showed typical flat REE patterns of shale, indicating that the redox state of the marine depositional environment has not changed much.

RSEs

The enrichment factors of trace elements are crucial indices for reconstructing paleoenvironmental conditions (Fig. 8).

In our study, distinctive enriched models in carbonates for RSEs (V, Ni, U, Mo, Cu, and Cd) and other major/trace elements (Fe, Mn, Co, and Li) were observed in the lower and upper parts of Kaiyang location, with rough locations at 84.6–452.36 m (Interval 2, Doushantuo and Dengying Formations) and 1089.50–1483.09 m (Interval 4, from Qingxudong Formation to Loushanguan Formation), respectively. In Interval 2, almost all of the elements, including V, Ni, U, Mo, Cu, Cd, Fe, Mn, Co, and Li, showed a high level of enrichment, and the enrichment factors in Dengying Formation were higher than those in Niutitang Formation. In Interval 4, the enrichment pattern changed and showed Mo, U, Cd, and Cu enrichment in this area. However, V, Ni, Fe, Mn, Li, and Co were not highly enriched.

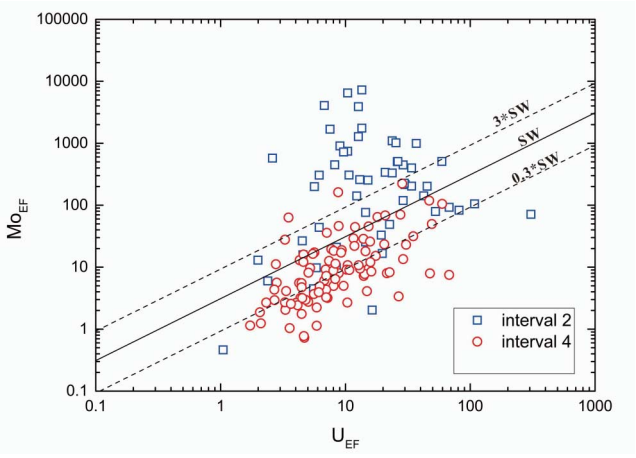

Fig. 9. Mo_{EF}-U_{EF} covariation patterns for carbonate samples in interval 2 and interval 4.

Algeo and Tribovillard (2009) proposed that the patterns of authigenic Mo-U covariation may prove useful in the analysis of specific redox conditions and processes in marine depositional systems. In our study, the samples in Intervals 2 and 4 showed distinct Mo_{EF}-U_{EF} patterns (Fig. 9).

The samples in Interval 2 exhibited high Mo_{EF}-U_{EF} ratio patterns (Mo/U ratio: 173.00, Mo_{EF}: 7266, U_{EF}: 13.5) to low Mo_{EF}-U_{EF} ratio patterns (Mo/U ratio: 0.25, Mo_{EF}: 2.6, U_{EF}: 3.3). This result suggests that shallow seawater in Interval 2 was oxidized gradually. The pattern in Interval 4 changed from low Mo_{EF}-U_{EF} ratio pattern (Mo/U ratio: 0.19, Mo_{EF}: 1.2, U_{EF}: 2.1) to high Mo_{EF}-U_{EF} ratio pattern (Mo/U ratio: 5.98, Mo_{EF}: 161.9, U_{EF}: 8.7). These values suggest that the shallow seawater in Interval 4 was suboxic/anoxic.

Algeo and Tribovillard (2009) reported that in an open marine system with expansive reducing bottom waters, Mo_{auth} accumulation exceeds that of U_{auth}, and the changed Mo/U ratio leads to a steep Mo_{EF} versus U_{EF} trend. The Mo_{EF}-U_{EF} pattern of Interval 4 is consistent with that in open marine conditions (Tribovillard *et al*., 2012). This consistency might be the reason for the proposition that the redox state of shallow seawater in Interval 4 was from oxic to anoxic.

Sr/Ba ratios

Sr/Ba ratios (Fig. 10) can trace eustatic changes (Sr/Ba ratio > 1 indicates a marine environment, 0.6 < Sr/Ba < 1 indicates a transition environment of land and sea, and Sr/Ba < 1 indicates a terrestrial environment) (Wang and Wu, 1983; Wang *et al*., 2017).

In our study, the Sr/Ba values in the strata changed

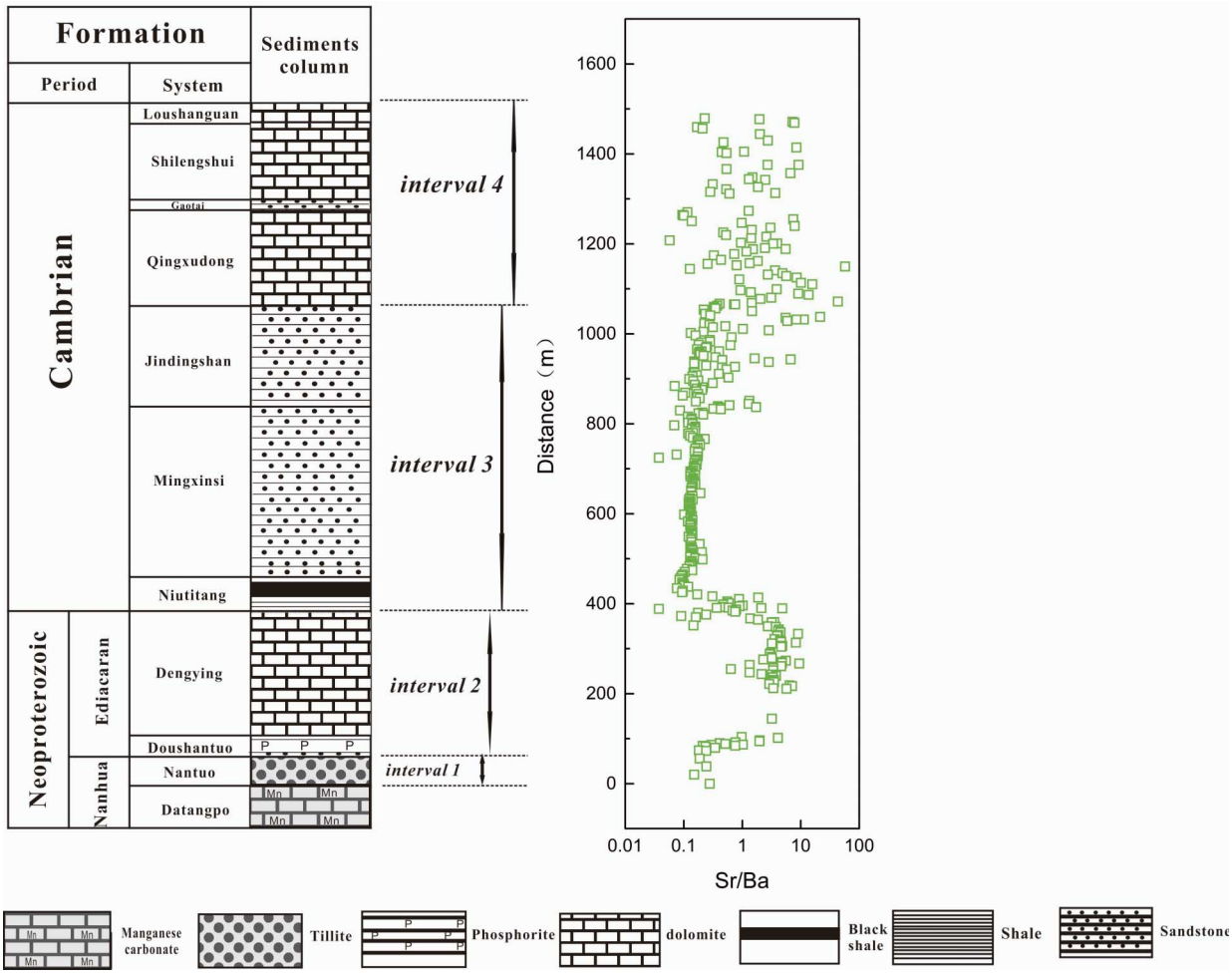

Fig. 10. Sr/Ba ratio of the Kaiyang Section.

several times from Doushantuo to Dengying Formation (mean = 0.7–3.4), from Niutitang to Mingxinsi Formation (mean = 1.0–0.10), from Mingxinsi to Jindingshan Formation (mean = 0.13–2), from Qingxudong to Gaotai Formation (mean = 7.36–0.1), and from Gaotai to Loushanguan Formation (mean = 0.1–3.48). These findings indicate that transgression/regression events may have occurred in this area at that time.

The Sr and Ba concentrations in the phosphorite samples from Doushantuo Formation varied greatly from 78.4 ppm to 1210 ppm and from 40.0 ppm to 2950 ppm, respectively. Sr and Ba exhibited higher abundance than Sr and Ba in normal seawater. The higher abundance values may be due to enrichment by various planktonic algae, indicating that microorganisms may have been involved in the formation of phosphorite in the study area.

The redox condition observed at Kaiyang location varied repeatedly between anoxic and oxic conditions during the sedimentation period from Interval 2 to Interval 4. This situation may be attributed to the fluctuation of the chemocline. In the study area, the enrichment factors of RSEs were coupled with the Sr/Ba ratio, which may indicate that the transgression/regression movement had a certain influence on the degree of enrichment. The upwelling generated by the strong transgression would have brought the reduced seawater from the bottom to the surface, and this might have caused the surface seawater to become increasingly reductive.

Implications for E-C transitional oceanic redox conditions

When the link between the foregoing geochemical data and the inferred redox conditions from REE are combined, the RSE enrichment factors in this study suggest that Nantuo Formation to Loushanguan Formation at the Kaiyang location might have undergone four intervals of evolution during the sedimentary period. Interval 1 is represented by sandstone during Nantuo Formation. The samples showed low RSE enrichment factors, no Ce anomaly, and low Y/Ho ratio (Fig. 11). The critical bioevents, eustatic change, and δCe of the Kaiyang Section are de-

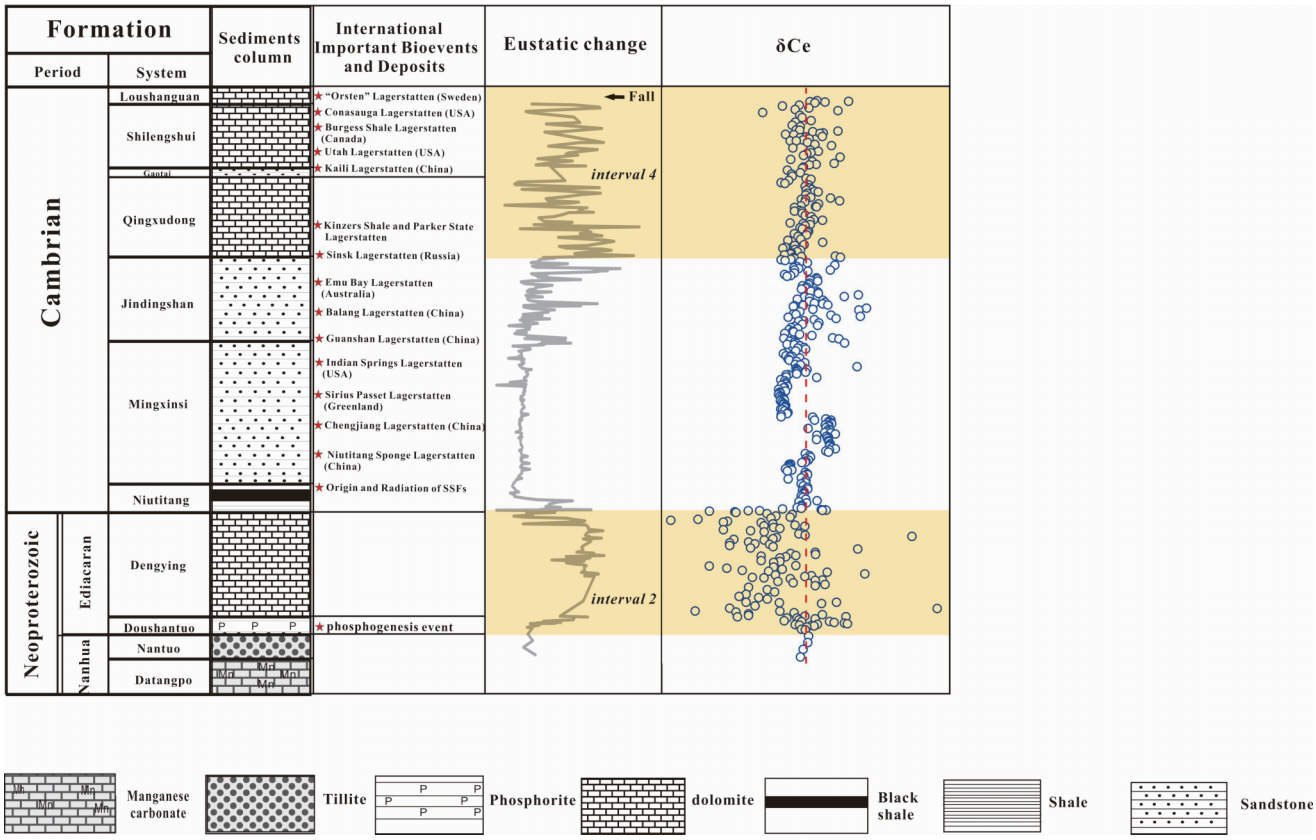

Fig. 11. Critical bioevents, eustatic change and δCe of the Kaiyang Section. Yellow shadows refer to distinctive redox-state from two carbonates intervals.

scribed in Fig. 11.

Interval 2 is represented by carbonates and phosphorites from Doushantuo Formation to Dengying Formation. They exhibited a fluctuating redox state of shallow water. The samples from Doushantuo Formation had no Ce anomaly, moderate Y/Ho ratios, and low enrichment factors. However, the samples from Dengying Formation showed obvious Ce anomaly, high Y/Ho ratios, high enrichment factors, and an oxidative Mo_{EF}-U_{EF} pattern. This condition reflects a change from anoxic to oxidized shallow seawater. Tribovillard *et al.* (2006) suggested that high RSE (e.g., V, Ni, U, Mo, and Cu) enrichment factors reflect sediments that were deposited in an anoxic/euxinic environment. However, in our study, all of the enrichment factors observed (V, Ni, U, Mo, Cu, Cd, Li, Fe, Mn, and Co) had high values. These changes in the ocean were probably caused by rising amounts of O_2 in the environment. Transgression occurred in Interval 2 along with an increase in sea level, and coastal oxidation may have been input to seawater, thus making seawater oxidized. This condition may indicate that these carbonates were deposited in an oxic/suboxic platform in shallow seawater, similar to modern seawater. It is consistent with records of Mo isotopes (Kendall *et al.*, 2015; Wen *et al.*, 2011, 2015) and near-zero $\delta^{56}Fe_{WR}$ values (Fan *et al.*, 2016).

Interval 3 is represented by black shale and sandstones from Niutitang to Jindingshan Formations. The samples showed low enrichment factors, weak or no Ce anomaly, and the lowest Y/Ho ratios. This condition represents a typical anoxic environment from Niutitang Formation, where black shale makes up the special deposits formed by rapid transgression at the turn from Neoproterozoic to Cambrian within the study area (Mei *et al.*, 2007). Transgression raised the oceanic redox interface and decreased the O_2 cycle of the atmosphere-ocean system. Therefore, the water column was anoxic, even euxinic (black shale). After this global "anoxic event," regression occurred in this interval, which is represented by argillutite and sandstone from Mingxinsi Formation to Jindingshan Formation. They chiefly formed two upward-shoaling depositional successions (marine regression) from argillutite of the shelf facies to sandstone of the littoral facies, and the sea level dropped relative to Niutitang Formation. Along with the sea level drop, the oceanic redox interface also dropped, thereby increasing the O_2

cycle of the atmosphere-ocean system. Although oxygen concentrations in the water column increased, they did not attain a high level at that time.

Interval 4 is represented by carbonates from Qingxudong to Loushanguan Formations. The samples were characterized by high RSE (U and Mo) enrichment factors but are different from those in Interval 2. Similarly, weak or no Ce anomaly, low Y/Ho ratios, and a reductive Mo_{EF}-U_{EF} pattern were observed. The Mo_{EF}-U_{EF} pattern in this interval is consistent with that under open marine conditions, which suggests that transgression enhanced the connectivity of the bottom anoxic water with the surface water. Large amounts of trace elements in the bottom water entered the surface water with the transgression, and the oceanic redox interface rose and cut off the connection with the atmosphere. This made the water column anoxic.

Conclusion

A preliminary ocean redox chemistry analysis was conducted using traditional REE methods (e.g., δCe, δEu, REE distribution pattern and Y/Ho) and the enrichment factors of the strata series in the shelf of Kaiyang location on the Ediacaran to the Cambrian Yangtze Platform. In combination with previously published geochemical data, our data suggest a fluctuant redox state of the Ediacaran to the Cambrian ocean, in which a fluctuant redox state of shallow water coexisted with eustatic change. Our analysis of Kaiyang samples indicated that seawater in the Ediacaran-Cambrian transition had δCe values < 0.6, Y/Ho ratios > 44, and the REE pattern was same as for modern seawater. This development in oceanic chemistry was likely similar to that of the modern ocean. This crucial oxygenation event appears to have occurred before the Cambrian stage, suggesting that large-scale oxygenation of the atmospheric-oceanic system may have played a critical role in the main phase of "Cambrian Explosion" and that a fluctuating redox state of shallow seawater existed during the Cambrian stage.

Acknowledgments—This work was financially supported by the Strategic Priority Research Program (B) of the Chinese Academy of Sciences (Grant No. XDB18030302) and National Science Foundation of China (41890841, 41773015, and U1812402). We also thank anonymous reviewer and editors (Yoshio Takahashi and Katsuhiko Suzuki) for improving the manuscript.

References

Algeo, T. J. and Tribovillard, N. (2009) Environmental analysis of paleoceanographic systems based on molybdenum-uranium covariation. *Chem. Geol*. **268**, 211–225.

Amthor, J. E., Grotzinger, J. P., Schroder, S., Bowring, S. A., Ramezani, J., Martin, M. W. and Matter, A. (2003) Extinction of Cloudina and Namacalathus at the Precambrian-Cambrian boundary in Oman. *Geology* **31**, 431–434.

Bau, M. and Dulski, P. (1999) Comparing yttrium and rare earths in hydrothermal fluids from the Mid-Atlantic Ridge: implications for Y and REE behavior during nearvent mixing and for the Y/Ho ratio of Proterozoic seawater. *Chem. Geol*. **155**, 77–90.

Bau, M., Koschinsky, A., Dulski, P. and Hein, J. R. (1996) Comparison of the partitioning behaviours of yttrium, rare earth elements, and titanium between hydrogenetic marine ferromanganese crusts and seawater. *Geochim. Cosmochim. Acta* **60**(10), 1709–1725.

Bau, M., Möller, P. and Dulski, P. (1997) Yttrium and lanthanides in eastern Mediterranean seawater and their fractionation during redox-cycling. *Mar. Chem*. **56**(1–2), 123–131.

Berner, R. A., Beerling, D. J., Dudley, R., Robinson, J. M., Wildman, J. and Richard, A. (2003) Phanerozoic atmospheric oxygen. *Annu. Rev. Earth Planet. Sci*. **31**, 105–134.

Byrne, R. H. and Sholkovitz, E. (1996) Marine chemistry and geochemistry of the lanthanides. *Handb. Phys. Chem. Rare Earths* **23**, 497–593.

Canfield, D. E., Poulton, S. W. and Narbonne, G. M. (2007) Late-neoproterozoic deep-ocean oxygenation and the rise of animal life. *Science* **315**(5808), 92–95.

Chang, H., Chu, X., Feng, L., Huang, J. and Chen, Y. (2018) Marine redox stratification on the earliest Cambrian (*ca*. 542–529 Ma) Yangtze platform. *Palaeogeogr. Palaeoclimatol. Palaeoecol*. **504**, 75–85.

Cook, P. J. (1992) Phosphogenesis around the Proterozoic-Phanerozoic transition. *J. Geol. Soc*. **149**(4), 615–620.

Cook, P. J. and Shergold, J. H. (1984) Phosphorus, phosphorites and skeletal evolution at the Precambrian-Cambrian bound-ary. Nature 308(5956), 231−236.

Dulski, P. (1994) Interferences of oxide, hydroxide and chloride analyte species in the determination of rare earth elements in geological samples by in-ductively coupled plasma-mass spectrometry. *Fresen. J. Anal. Chem.* **350**(4−5), 194−203.

Douville, E., Bienvenu, P., Charlou, J. L., Donval, J. P., Fouquet, Y., Appriou, P. and Gamo, T. (1999) Yttrium and rare earth elements in fluids from various deep-sea hydrothermal systems. *Geochim. Cosmochim. Acta* **63**, 627–643.

Elderfield, H., Hawkesworth, C. J., Greaves, M. J. and Calvert, S. (1981) Rare earth element geochemistry of oceanic ferromanganese nodules. *Geochim. Cosmochim. Acta* **45**(4), 513–528.

Fan, H., Wen, H. and Zhu, X. (2016) Marine redox conditions in the Early Cambrian ocean: Insights from the Lower Cambrian Phosphorite Deposits, South China. *J. Earth Sci*. **27**(2), 282–296.

Feng, L., Li, C., Huang, J., Chang, H. and Chu, X. (2014) A sulfate control on marine middepth euxinia on the early Cambrian (*ca*. 529–521 Ma) Yangtze platform, South China. *Precambrian Res*. **246**, 123–133.

Fike, D. A., Grotzinger, J. P., Pratt, L. M. and Summons, R. E. (2006) Oxidation of the Ediacaran Ocean. *Nature* **444**(7120),

744–747.

German, C. R., Holliday, B. P. and Elderfield, H. (1991) Redox cycling of rare earth elements in the suboxic zone of the Black Sea. *Geochim. Cosmochim. Acta* **55**(12), 3553–3558.

Guo, Q., Strauss, H., Liu, C., Goldberg, T., Zhu, M., Pi, D., Heubeck, C., Vernhet, E., Yang, X. and Fu, P. (2007) Carbon isotopic evolution of the terminal Neoproterozoic and early Cambrian: evidence from the Yangtze Platform, south China. *Palaeogeogr. Palaeoclimatol. Palaeoecol*. **254**, 140–157.

Jiang, G. Q., Shi, X. Y., Zhang, S. H., Wang, Y. and Xiao, S. H. (2011) Stratigraphy and paleogeography of the Ediacaran Doushantuo Formation (*ca*. 635–551 Ma) in South China. *Gondwana Res*. **19**(4), 831–849.

Jiang, S. Y., Zhao, H. X., Chen, Y. Q., Yang, T., Yang, J. H. and Ling, H. F. (2007) Trace and rare earth element geochemistry of phosphate nodules from the lower Cambrian black shale sequence in the Mufu Mountain of Nanjing, Jiangsu province, China. *Chem. Geol*. **244**(3), 584–604.

Kendall, B., Komiya, T., Lyons, T. W., Bates, S. M., Gordon, G. W., Romaniello, S. J. *et al*. (2015) Uranium and molybdenum isotope evidence for an episode of widespread ocean oxygenation during the late Ediacaran period. *Geochim. Cosmochim. Acta* **156**, 173–193.

Kholodov, V. and Butuzova, G. Y. (2001) Problems of iron and phosphorus geochemistry in the Precambrian. *Lithol. Miner. Resour*. **36**(4), 291–302.

Klinkhammer, G. P., Elderfield, H., Edmond, J. M. and Mitra, A. (1994) Geochemical implications of rare earth element patterns in hydrothermal fluids from midocean ridges. *Geochim. Cosmochim. Acta* **58**, 5105–5113.

Landing, E. (2004) Precambrian-Cambrian boundary interval deposition and the marginal platform of the Avalon microcontinent. *J. Geodyn*. **2004**, 411–435.

Lawrence, M. G. and Kamber, B. S. (2006) The behaviour of the rare earth elements during estuarine mixing-revisited. *Mar. Chem*. **100**(1–2), 147–161.

Lehmann, B., Frei, R., Xu, L. and Mao, J. (2016) Early Cambrian black shale-hosted Mo-Ni and V mineralization on the rifted margin of the Yangtze Platform, China: reconnaissance chromium isotope data and a refined metallogenic model. *Econ. Geol*. **111**, 89–103.

Li, C., Love, G. D., Lyons, T. W., Fike, D. A., Sessions, A. L. and Chu, X. (2010) A stratified redox model for the Ediacaran ocean. *Science* **328**(5974), 80–83.

Ling, H. F., Chen, X., Li, D., Wang, D., Shields-Zhou, G. A. and Zhu, M. Y. (2013) Cerium anomaly variations in Ediacaran-earliest Cambrian carbonates from the Yangtze Gorges area, South China: Implications for oxygenation of coeval shallow seawater. *Precambrian Res*. **225**, 110–127.

McArthur, J. M. and Walsh, J. N. (1984) Rare-earth geochemistry of phosphorites. *Chem. Geol*. **47**(3–4), 191–220.

McLennan, S. M. (1989) Rare earth elements in sedimentary rocks; influence of provenance and sedimentary processes. *Rev. Miner. Geochem*. **21**(1), 169–200.

McLennan, S. M. (2001) Relationships between the trace element composition of sedimentary rocks and upper continental crust. *Geochem. Geophys. Geosyst*. **2**, 203–236.

Mei, M. X., Ma, Y. S., Zhang, H., Meng, X. Q. and Chen, Y. H. (2007) Sequencestratigraphic framework for the Cambrian of the Upper Yangtze region: Ponder on the sequence stratigraphic background of the Cambrian biological diversity events. *J. Stratigraphy* **31**, 68–78 (in Chinese).

Mi, W. T. (2010) Phosphorites' Sedimentary Event in Sinian Doushantuo period West Yangtze Area—the Cases Study of Weng'an Phosphorite in Guizhou and Yichang Phosphorite in Hubei [D]. Chengdu Univ. Technol., Chengdu (in Chinese).

Nothdurft, L. D., Webb, G. E. and Kamber, B. S. (2004) Rare earth element geochemistry of Late Devonian reefal carbonates, Canning Basin, Western Australia: confirmation of a seawater REE proxy in ancient limestones. *Geochim. Cosmochim. Acta* **68**(2), 263–283.

Nozaki, Y., Zhang, J. and Amakawa, H. (1997) The fractionation between Y and Ho in the marine environment. *Earth Planet. Sci. Lett*. **148**(1–2), 329–340.

Och, L. M. and Shields-Zhou, G. A. (2012) The Neoproterozoic oxygenation event: environmental perturbations and biogeochemical cycling. *Earth-Sci. Rev*. **110**, 26–57.

Ohta, A. and Kawabe, I. (2001) REE(III) adsorption onto Mn dioxide (δ-MnO_2) and Fe oxyhydroxide: Ce(III) oxidation by δ-MnO_2. *Geochim. Cosmochim. Acta* **65**(5), 695–703.

Planavsky, N. J., Rouxel, O. J., Bekker, A., Lalonde, S. V., Konhauser, K. O., Reinhard, C. T. and Lyons, T. W. (2010) The evolution of the marine phosphate reservoir. *Nature* **467**(7319), 1088–1090.

Schroder, S. and Grotzinger, J. P. (2007) Evidence for anoxia at the Ediacaran-Cambrian boundary: the record of redox-sensitive trace elements and rare earth elements in Oman. *J. Geol. Soc*. **164**, 175–187.

Scott, C., Lyons, T. W., Bekker, A., Shen, Y., Poulton, S. W., Chu, X. and Anbar, A. D. (2008) Tracing the stepwise oxygenation of the Proterozoic ocean. *Nature* **452**(7186), 456–459.

Shields, G. and Stille, P. (2001) Diagenetic constraints on the use of cerium anomalies as palaeoseawater redox proxies: An isotopic and REE study of Cambrian phosphorites. *Chem. Geol*. **175**(1–2), 29.

Shields-Zhou, G. and Och, L. (2011) The case for a Neoproterozoic Oxygenation Event: geochemical evidence and biological consequences. *GSA Today* **21**, 4–11.

Sholkovitz, E. R., Landing, W. M. and Lewis, B. L. (1994) Ocean particle chemistry: the fractionation of rare earth elements between suspended particles and seawater. *Geochim. Cosmochim. Acta* **58**(6), 1567–1579.

Slack, J. F., Grenne, T., Bekker, A., Rouxel, O. J. and Lindberg, P. A. (2007) Suboxic deep seawater in the late Paleoproterozoic: Evidence from hematitic chert and iron formation related to seafloor-hydrothermal sulfide deposits, central Arizona, USA. *Earth Planet. Sci. Lett*. **255**(1), 243–256.

Steiner, M., Wallis, E., Erdtmann, B. D., Zhao, Y. L. and Yang, R. D. (2001) Submarine-hydrothermal exhalative ore layers in black shales from south China and associated fossils—insights into a lower Cambrian facies and bio-evolution. *Palaeogeogr. Palaeoclimatol. Palaeoecol*. **169**(3–4), 165–191.

Tachikawa, K., Jeandel, C., Vangriesheim, A. and Dupre, B. (1999) Distribution of rare earth elements and neodymium isotopes in suspended particles of the tropical Atlantic Ocean (EUMELI site). *Deep-Sea Res. Part I* **46**, 733–755.

Takahashi, Y., Shimizu, H., Usui, A., Kagi, H. and Nomura, M. (2000) Direct observation of tetravalent cerium in ferromanganese nodules and crusts by X-ray-absorption near-edge structure (XANES). *Geochim. Cosmochim. Acta*, **64**, 2929–2935.

Tanaka, K., Tani, Y., Takahashi, Y., Tanimizu, M., Suzuki, Y., Kozai, N. and Ohnuki, T. (2010) A specific Ce oxidation process during sorption of rare earth elements on biogenic Mn oxide produced by Acremonium sp. strain KR21-2. *Geochim. Cosmochim. Acta* **74**(19), 5643–5477.

Tribovillard, N., Algeo, T. J., Lyons, T. and Riboulleau, A. (2006) Trace metals as paleoredox and paleoproductivity proxies: An update. *Chem. Geol*. **232**, 12–32.

Tribovillard, N., Algeo, T. J., Baudin, F. and Riboulleau, A. (2012) Analysis of marine environmental conditions based on molybdenum-uranium covariation-applications to Mesozoic paleooceanography. *Chem. Geol*. **324–325**, 46–58.

Wang, F., Li, X., Deng, X., Li, Y., Tian, J., Li, S. and You, J. (2017) Geochemical characteristics and environmental implications of trace elements of Zhifang Formation in Ordos Basin. *J. Stratigraphy* **35**(6), 1265–1273 (in Chinese).

Wang, Y. and Wu, P. (1983) Geochemical indicators of sediments in the coastal zone of Jiangsu and Zhejiang Provinces. *J. Tongji Uni*. **4**, 82–90 (in Chinese).

Webb, G. E. and Kamber, B. S. (2000) Rare earth elements in Holocene reefal microbialites: A new shallow seawater proxy. *Geochim. Cosmochim. Acta* **64**(9), 1557–1565.

Wen, H., Carignan, J., Zhang, Y., Fan, H., Cloquet, C. and Liu, S. (2011) Molybdenum isotopic records across the Precambrian-Cambrian boundary. *Geology* **39**(8), 775–778.

Wen, H., Fan, H., Zhang, Y., Cloquet, C. and Carignan, J. (2015) Reconstruction of early Cambrian ocean chemistry from mo isotopes. *Geochim. Cosmochim. Acta* **164**, 1–16.

Wille, M., Nagler, T. F., Lehmann, B., Schroder, S. and Kramers, J. D. (2008) Hydrogen sulphide release to surface waters at the Precambrian/Cambrian boundary. *Nature* **453**(7196), 767–769.

Xiang, L., Schoepfer, S. D., Shen, S. Z., Cao, C. Q. and Zhang, H. (2017) Evolution of oceanic molybdenum and uranium reservoir size around the Ediacaran-Cambrian transition: evidence from western Zhejiang, south China. *Earth Planet. Sci. Lett*. **464**, 84–94.

Xu, L., Lehmann, B., Mao, J., Nägler, T. F., Neubert, N., Böttcher, M. E. and Escher, P. (2012) Mo isotope and trace element patterns of lower Cambrian black shales in south China: multi-proxy constraints on the paleoenvironment. *Chem. Geol*. **318**, 45–59.

Zhang, J., Amakawa, H. and Nozaki, Y. (1994) The comparative behaviors of yttrium and lanthanides in the seawater of the north Pacific. *Geophys. Res. Lett*. **21**, 2677–2680.

Zhu, B., Jiang, S. Y., Yang, J. H., Pi, D. H., Ling, H. F. and Chen, Y. Q. (2014) Rare earth element and Sr-Nd isotope geochemistry of phosphate nodules from the lower Cambrian Niutitang Formation, NW Hunan Province, South China. *Palaeogeogr. Palaeoclimatol. Palaeoecol*. **398**, 132–143.

Zhu, M., Zhang, J. and Yang, A. (2007) Integrated Ediacaran (Sinian) chronostratigraphy of South China. *Palaeogeogr. Palaeoclimatol. Palaeoecol*. **254**, 7–61.

Supplementary Materials

URL (http://www.terrapub.co.jp/journals/GJ/archives/data/54/MS607.pdf)
Tables S1 and S2